Effect of microstructure on the fatigue properties of Ti–6Al–4V titanium alloys

G.Q. Wu [a,*], C.L. Shi [a], W. Sha [b], A.X. Sha [c], H.R. Jiang [a]

[a] School of Materials Science and Engineering, Beihang University, 37 Xueyuan Road, Haidian District, Beijing 100191, China
[b] School of Planning, Architecture and Civil Engineering, Queen's University Belfast, Belfast BT7 1NN, UK
[c] Beijing Institute of Aeronautical Materials, Beijing 100095, China

ARTICLE INFO

ABSTRACT

Through an analysis on microstructure and high cycle fatigue (HCF) properties of Ti–6Al–4V alloys which were selected from literature, the effects of microstructure types and microstructure parameters on HCF properties were investigated systematically. The results show that the HCF properties are strongly determined by microstructure types for Ti–6Al–4V. Generally the HCF strengths of different microstructures decrease in the order of bimodal, lamellar and equiaxed microstructure. Additionally, microstructure parameters such as the primary α (α_p) content and the α_p grain size in bimodal microstructures, the α lamellar width in lamellar microstructure and the α grain size in equiaxed microstructures, can influence the HCF properties.

© 2012 Elsevier Ltd. All rights reserved.

1. Introduction

Due to their excellent properties (high specific strength, high fatigue strength, good corrosion resistance, etc.), titanium components (particularly Ti–6Al–4V) are often used for manufacturing critical systems such as airfoils, undercarriage components, and airframes [1–4] instead of heavy steel components. During these applications titanium structures are often exposed to fatigue loading [1]. Fatigue fracture is an important failure mode for these structures [5].

Depending on the alloy class, the parameters possibly having an influence on the fatigue life of titanium alloys include grain size (phase dimension and morphology), age hardening condition, degree of work hardening, elastic constants, and crystallographic texture [1]. Depending on the thermomechanical treatment or heat treatment of the ($\alpha + \beta$) titanium alloy, such as Ti–6Al–4V, the microstructure and mechanical properties can vary in a wide range [3,6]. Such influences have been documented in numerous reports in the literature [4,7–11]. However, due to experimentation limitations, experimental results are not always reproducible, and thus it is difficult to compare among fatigue properties obtained from different tests, even for a same microstructure. There has not been enough data to correlate fatigue properties based on differing microstructures. Based on the comparison of microstructure types of Ti–6Al–4V alloys, Hines and Nalla [12,13] pointed out that lamellar microstructure had higher HCF strength than bimodal microstructure. However, Zuo et al. [10] and Niinomi et al. [14] ob-

tained the opposite result. Ivanova et al. [15] and Peters and Lütjering [16,17] proved that bimodal microstructure had higher HCF strength than the equiaxed microstructure, and Peters and Lütjering [17] showed that lamellar microstructure also had higher HCF strength than the equiaxed microstructure. However, it was also reported [2] that equiaxed microstructure had the highest HCF strength, and according to Ivanova and Adachi [18,19], lamellar microstructure had a similar HCF strength to bimodal microstructure. The reasons for this contradiction have not been well explained. Additionally, the fatigue strength would be dependent on microstructural parameters of each Ti–6Al–4V alloy, such as the α_p content and α_p grain size in bimodal microstructure [15,18,20], the α grain size in the equiaxed microstructure [2,18,21], and the lamellar α width in lamellar microstructure [10,12,13].

So, there is differing information in the literature concerning the relative strengths of Ti–6Al–4V alloys based on microstructure type. These authors did not necessarily use the same bimodal, lamellar, and equiaxed microstructures. These differences can make sense if we incorporate the parameters that are listed.

However, the influence of the microstructural parameters on fatigue property is difficult to investigate systematically, because the fatigue test costs a lot of human and material resources. A more comprehensive evaluation of the influence of the individual microstructure parameters on fatigue properties is difficult, because all data presented in a paper are from one research group. This also limits the ability to evaluate additional effects due to variations in specimen preparation, test procedure, micro-alloy composition differences, heat treatment, rolling or forging procedure affecting texture, etc. [22].

* Corresponding author. Tel./fax: +86 1082313240.
E-mail address: guoqingwu@buaa.edu.cn (G.Q. Wu).

Through an analysis on microstructures and HCF strengths of the Ti–6Al–4V alloys based on the literature dated from 1972 to present, effects of microstructure types and microstructure parameters on HCF properties were investigated systematically. The influences of the microstructure types (bimodal, lamellar, equiaxed) on the HCF properties were investigated. Additionally, the effects of the microstructure parameters (α_p content and α_p grain size, lamellar width) on the HCF properties were investigated.

2. Method

In this paper, 75 sets of data in 21 references [10,12–15,17–21,23–33] were collected with information about the HCF strength data and microstructure parameters of Ti–6Al–4V alloys according to microstructure types (Fig. 1 and Tables 1–3). No testing was done by the authors but the work relied entirely on the literature data. All fatigue tests were performed in room-temperature air under axial loading conditions with a sine wave on smooth-bar, unnotched hourglass specimens.

Most of the microstructural parameters (α_p content, α_p grain size and lamellar width) can be obtained from literature, but the ones that are not given clearly are analyzed by the Nano Measurer1.2 software according to the SEM images in the references. All these measured parameters are labelled as 'a' in Tables 1–3. α grain size was measured by linear intercept method [34], and α lamellar width was measured by the way described in [35]. Fatigue strength data were obtained from the stress–life (S–N) curves in the literature.
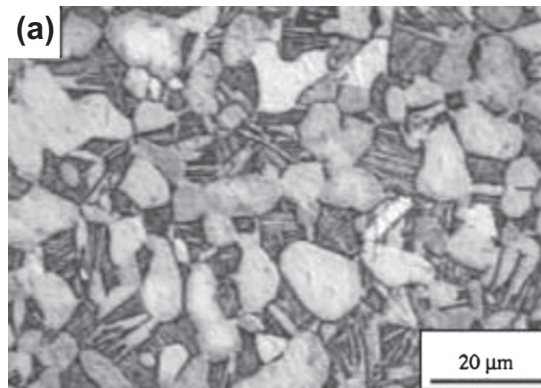

(a) bimodal [10]

(b) equiaxed [24]
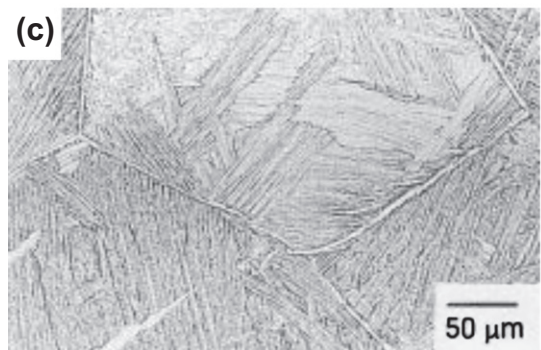
(c) lamellar [12]

Fig. 1. Three typical microstructures.

Table 1
Database of bimodal microstructure parameters and HCF data of Ti–6Al–4V alloys.

No.	Ref.	Bimodal (µm)		Frequency (Hz)	Stress ratio (R)	HCF strength (MPa)		
		V_α	D_α			10^5	10^6	10^7
1	Bellows et al. [25]	60	13[a]	60	−1	450	400	390
					0.1	667	611	556
					0.5	860	800	640
					0.8	950	920	900
2	Hines and Lütjering [12]	35	7.5[a]	90	−1	545	470	445
3	Ivanova et al. [15]	60.5	8	30	0.1	–	–	467
		24.8	8.5			830 (3×10^4)	620 (2×10^6)	550
4	Nalla et al. [13]	64	20	25	0.1	700	600	540[b]
					0.5	850	780	640[b]
5	Peters and Lütjering [17]	60	20	90	−1	480	400	375
6	Zuo et al. [10]	55	10	20,000	−1	–	546	518
7	Oguma and Nakamura [20]	–	4	120	0.1	900	865	850
		–	10			860	810	650
8	Nagai et al. [26]	–	4	20	0.01	800	720	640
		–	4[c]			800	720	690
		–	2.8			800	740	720
9	Broichhausen and Kann [27]	–	–	–	−1	588	547	539
10	Peters et al. [21]	–	6	80	−1	710	675	675
11	Hines et al. [28]	–	9.7[a]	90	−1	470	400	380
		–			0.1	700	550	500
		–			0.5	–	–	650
12	Ivanova et al. [18]	60.5	8	30	−1	462	441	414
		24.8	8.5			455	421	407
		28.7	5.5			510	497	490
		60.5	8		0.1	720	582	491
		24.8	8.5			720	613	551
		28.7	5.5			798	751	720
13	Rudinger and Fischer [29]	20[c]	–	130	0	725	700	680
			–			–	775	580
		50	–			700	590	480
14	Adachi et al. [19]	40[c]	10	90	−1	–	–	550
					0.2	–	–	700
					−1	–	–	540
					0.2	–	–	600
			6		−1	–	790	770
					0.2	1125	1075	1050
					−1	740	730	730
					0.2	1100	875	800
15	Nalla et al. [30]	64	20	5	−1	450		
16	Nakanura et al. [31]	–	4	120	−1	660	660	660
		–			−0.5	827	827	827
		–			0.1	911	878	844
17	Zuo et al. [32]	55	10	25	−1	570	530	–

[a] Measured by the authors.
[b] Frequency is 1000 Hz.
[c] Fatigue specimens with different textures.

Table 2
Database of equiaxed microstructure parameters and HCF data of Ti–6Al–4V alloys.

No.	Ref.	α grain size (μm)	Frequency (Hz)	Stress ratio (R)	HCF strength (MPa)		
					10^5	10^6	10^7
1	Hines and Lütjering [12]	2.5[a]	90	−1	550	505	485
2	Nalla et al. [13]	1.5[a]	25	0.1	710	610	570
				0.5	860	800	740
3	Zuo et al. [10]	1.5[a]	20,000	−1		533	492
4	Ivanova et al. [18]	0.92	30	−1	510	490	483
				0.1	782	736	704
5	Rudinger and Fischer [29]	–	130	0	700	660	600
		–			660	620	620
		–			690	660	660
6	Adachi et al. [19]	0.5	90	−1	740	690	680
				0.2	–	1050	1000
7	Niinomi et al. [14]	1.5[a]	10	0.1	750	660	600

[a] Measured by the authors.

Table 3
Database of lamellar microstructure parameters and HCF data of Ti–6Al–4V alloys.

No.	Ref.	Lamellar width (μm)	Frequency (Hz)	Stress ratio (R)	HCF strength (MPa)		
					10^5	10^6	10^7
1	Peters et al. [23]	1.5[b]	80	−1	650	630	620
					750	730	720
					700	690	690
					660	630	625
					620	590	590
2	Morrissey et al. [24]	5.7[a]	70	0.1	–	–	722
			400		–	–	778
			70	0.5	–	–	800
			400		–	–	880
			1800		–	–	1040
			70	0.8	–	–	1000
			400		–	–	1000
3	Ivanova et al. [15]	6.8	30	0.1	830 (3.5×10^5)	–	467
		8.5			830 (2.4×10^5)	620 (3×10^6)	451
4	Peters et al. [21]	2	80	−1	650	625	620
		12			530	500	500
5	Ivanova et al. [18]	6.8	30	−1	483	435	400
		8.5			421	393	366
		6.8		0.1	689	536	444
		8.5			673	551	476

[a] Measured by the authors.
[b] Fatigue specimens with different textures.

3. Results

According to the different fatigue life (10^5, 10^6 and 10^7 cycles), the fatigue strengths of Ti–6Al–4V alloys with three typical microstructures (bimodal, lamellar and equiaxed) are presented in Fig. 2. The exponential curve fitting is used to show the trend and comparison of the data. Other types of curve could have been used, but they are expected to show similar trend and comparison. Due to the large scatter of the data, a comparison using the mean and standard deviation of the HCF strength based on the three
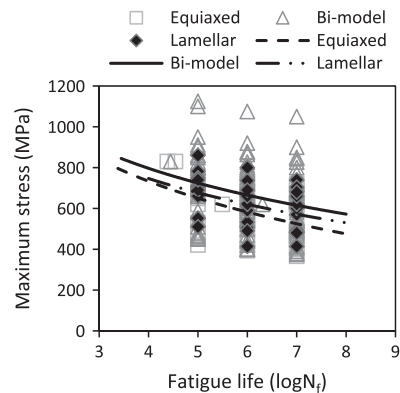

Fig. 2. HCF properties of Ti–6Al–4V alloy with three typical microstructures.

types of microstructures would not be meaningful, as there will be huge standard deviation values, making it apparent that the means overlap. It can be demonstrated that the HCF strength of the three typical microstructures is dispersive and overlapped, but as a whole, the bimodal data appear above, then lamellar and the equiaxed ones distribute at the bottom. It can be seen from the S–N curves that the fatigue life increases as the loading decreases. Generally the HCF strength of different microstructures decreases in the order of bimodal, lamellar and equiaxed microstructure.

3.1. Bimodal microstructure

The effect of α_p volume fraction (V_α) and α_p size of Ti–6Al–4V alloy with bimodal microstructures on the HCF properties are shown in Figs. 3 and 4, respectively. Fig. 3a–c shows the analysis results of HCF strength at 10^5, 10^6 and 10^7 cycles, respectively. It can be seen that the fatigue strength is highest when V_α is in the range of 30–50%. For the convenience of comparison, Fig. 3d divides the data into three groups according to the α_p volume fraction. e.g., $V_\alpha < 30\%$, $V_\alpha = 30–50\%$ and $V_\alpha > 50\%$. From the average data (Fig. 3d), the group of $V_\alpha = 30–50\%$ has the highest HCF strength. It can be seen that the HCF strength of Ti–6Al–4V alloys with bimodal microstructures will increase at first and then decrease with the increasing α_p volume fraction. By visually looking at the individual cases, it would appear that most data is similar, with some outliers in the 30–50% region. Fig. 3d was obtained by averaging. It summarises available data, but should not be used for quantitative prediction. When presenting individual cases, we deliberately do not differentiate sources of data, so as to treat all sources equally. For example, there seems to exist really high data at $V_\alpha = 40\%$, but we do not go into details of examining whether they are all from one alloy or reference.

The HCF strength of Ti–6Al–4V alloys with bimodal microstructures as a function of the α_p size is shown in Fig. 4. Fig. 4a–c shows the analysis results of HCF strength at 10^5, 10^6 and 10^7 cycles, respectively. It can be seen that all data have some dispersion, but in general the fatigue strength decreases with the increasing of α_p size from 2.8 μm to 20 μm. For the convenience of comparison, Fig. 4d divides the data into three groups according to the α_p size, e.g., $D_\alpha < 5$ μm, $D_\alpha = 5–10$ μm and $D_\alpha > 10$ μm. It can be seen from Fig. 4d that the HCF strength of Ti–6Al–4V alloys with bimodal microstructures declines apparently with the increasing of α_p size from 2.8 to 20 μm. It should be noted that Fig. 4d was obtained by averaging. There are individual cases apparently against the trend shown in Fig. 4d. One should resist the temptation of making a quick conclusion by visually looking at individual cases, which was why averaging is used here. Note also that the range division, i.e., $D_\alpha < 5$ μm, $D_\alpha = 5–10$ μm and $D_\alpha > 10$ μm, is somewhat arbitrary, and there
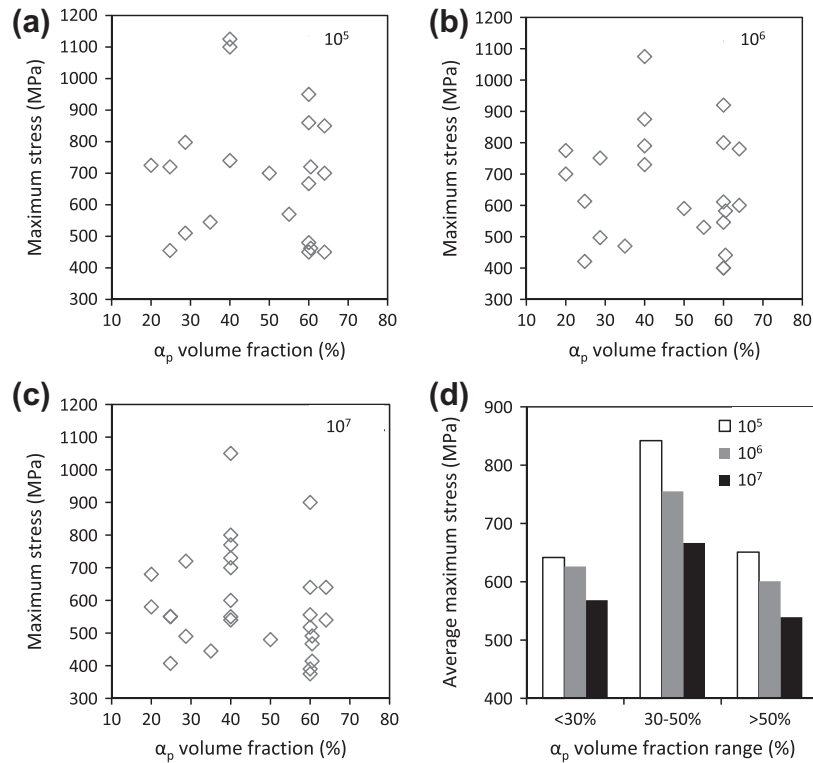
Fig. 3. HCF strength of Ti–6Al–4V alloys with bimodal microstructure at different α_p volume fractions: (a) 10^5 cycles, (b) 10^6 cycles, (c) 10^7 cycles and (d) analysis in groups.
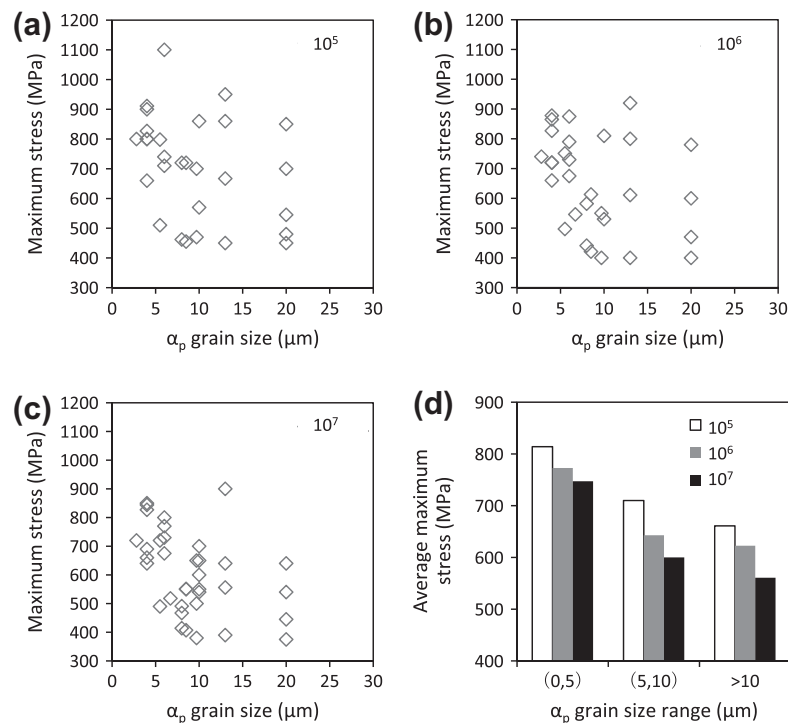

Fig. 4. HCF strength of Ti–6Al–4V alloy with bimodal microstructure at different α_p size: (a) 10^5 cycles, (b) 10^6 cycles, (c) 10^7 cycles and (d) analysis in groups.

is actually no data for D_α = 5 μm exactly. Different results may be obtained by dividing the range differently.

3.2. Equiaxed microstructure

Fig. 5 gives the correlation between HCF strength and α grain size of Ti–6Al–4V alloys with equiaxed microstructure. Fig. 5a–c

shows the analysis results of HCF strength at 10^5, 10^6 and 10^7-cycles, respectively. It can be seen that, both the HCF strength at 10^5 (Fig. 5a) and 10^6 (Fig. 5b) cycles decrease when the average α grain size increases. However, there are some sets of extremely high HCF strength data around 10 μm grain size, as illustrated in Fig. 5c. The literature containing this data only tested the HCF strength at

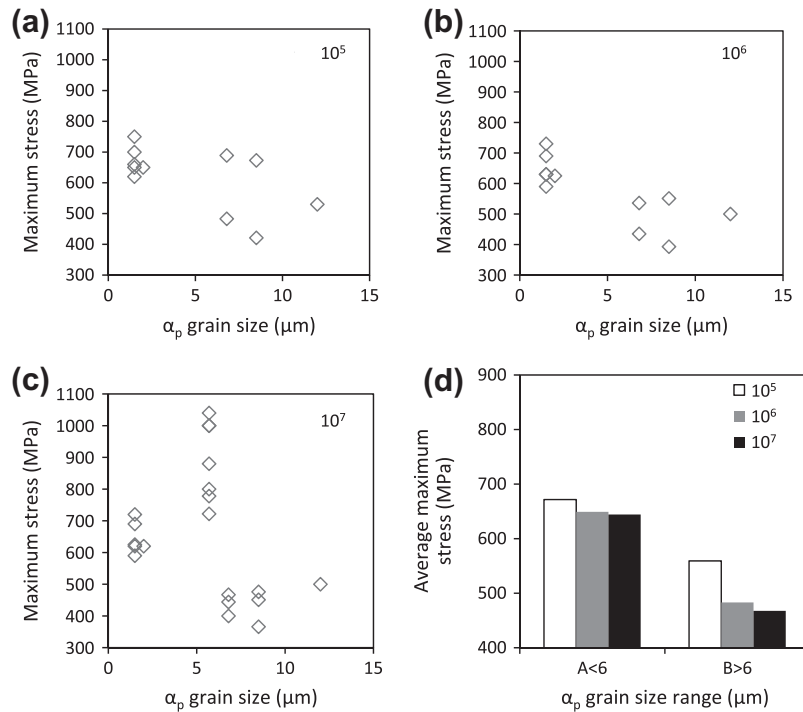**Fig. 5.** HCF strength of Ti–6Al–4V alloy with equiaxed microstructure at different α grain size: (a) 10^5 cycles, (b) 10^6 cycles, (c) 10^7 cycles and (d) analysis in groups.
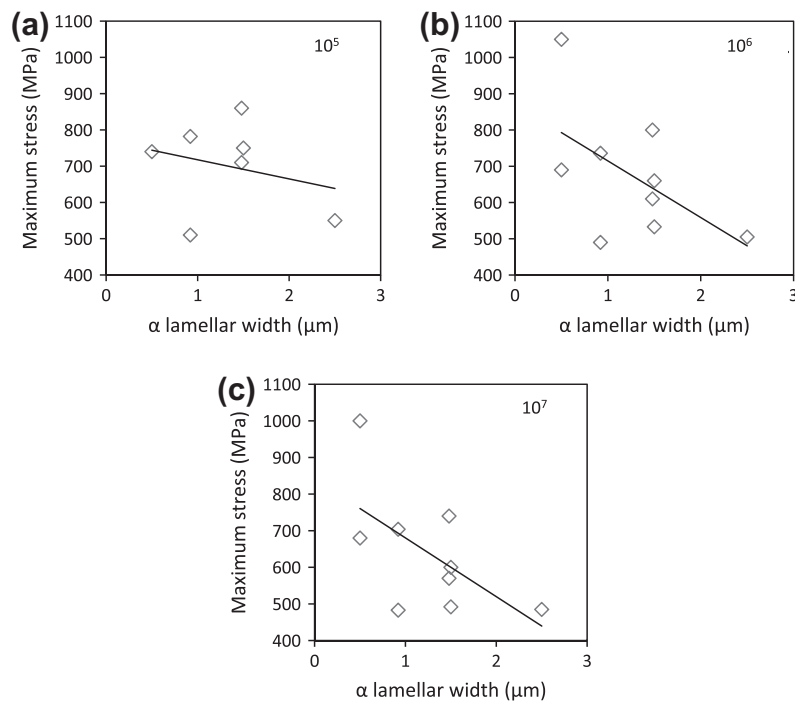

Fig. 6. HCF strength of Ti–6Al–4V alloy with lamellar microstructure at different α lamellar width: (a) 10^5 cycles, (b) 10^6 cycles and (c) 10^7 cycles.

10^7 cycles. For the convenience of comparison, these six extremely high data in Fig. 5c are eliminated and the data are divided into two groups according to 6 μm grain size, as shown in Fig. 5d. It can be seen that, the average HCF strength of the group with α grain size less than 6 μm (including 6 μm) is larger than that of the other one.

3.3. Lamellar microstructure

Fig. 6 gives the connection between the HCF strength and α lamellar width of Ti–6Al–4V alloys with lamellar microstructure. The linear curve fitting is used to show the trend of the data. Other types of curve could have been used, but they are expected to show

a similar trend. From both the limited results and fitting lines (not good fits to the data) of HCF strength at 10^5, 10^6 and 10^7 cycles, respectively, the HCF strength declines with the increasing of α lamellar width. It should be noted that these fitting lines are not good fits to the data, but are used to show trends.

4. Discussion

From all the results above, the HCF strength of the Ti–6Al–4V alloy with three typical microstructures may overlap among themselves in some ranges because of the limited material manufacturing industry [36]. However, generally the HCF strengths of different microstructures decrease in the order of bimodal, lamellar and equiaxed microstructure [37]. Though the conclusion of the bimodal microstructures having best high cycle fatigue is in contradiction with some literature, there are also ample explanation on the effect of bimodal structure on the crack growth [38], and statements that the bimodal structure generally ensures good fatigue endurance of the Ti–6Al–4V alloy [39] and a bimodal grain structure seems beneficial [40]. These references should be consulted for discussions on the mechanisms. Experimentally, bimodal Ti–6Al–4V alloys with best high fatigue properties has been found in many publications used to develop the analysis in this paper, as well as in publications not used, for example [39]. Therefore, it will be much more beneficial to choose bimodal microstructure if the work pieces need strict fatigue properties. Manufacturers can optimize the HCF strength of bimodal microstructures by controlling the α_p volume fraction and α_p size, respectively. From the present analysis results, it is beneficial to choose the microstructure with α_p volume fraction ranging from 30% to 50% and α_p size as small as possible. For equiaxed or lamellar microstructures, the HCF strength can be controlled by α grain size or α lamellar width [37,41]. However, due to the limited data, there is no definite conclusion. Therefore this work will continue until definite conclusions are drawn from the increasing database in the future.

5. Conclusion

Through an analysis on the microstructures and HCF strengths of Ti–6Al–4V alloys which dated from 1972 to date, the effects of microstructure types and microstructure parameters on the HCF strength were investigated systematically. Based on this analysis, the following conclusions can be drawn:

(1) The microstructure types of Ti–6Al–4V alloy have significant influence on the HCF strength. Generally the HCF strengths of different microstructures decrease in the order of bimodal, lamellar and equiaxed microstructure.
(2) The primary α content and grain size in bimodal microstructure of Ti–6Al–4V alloy have significant influence on the HCF strength. The HCF strength increases at first, then declines with the increasing of the α_p volume fraction, and the HCF strength decreases with the increasing of the α_p size.
(3) The α grain size in equiaxed microstructure or α lamellar width in lamellar microstructure has significant influence on the HCF strength. The HCF strength declines with the increasing of either α grain size or α lamellar width.

Acknowledgements

References

[1] Leyens C, Peters M, editors. Titanium and titanium alloys: fundamentals and applications. Weinheim: Wiley-VCH; 2003.
[2] Lütjering G, Williams JC. Titanium. 2nd ed. New York, Berlin, Heidelberg: Springer; 2007.
[3] Oberwinkler B, Riedler M, Eichlseder W. Importance of local microstructure for damage tolerant light weight design of Ti–6Al–4V forgings. Int J Fatigue 2010;32:808–14.
[4] Knobbe H, Köster P, Christ H, Fritzen C, Riedler M. Initiation and propagation of short fatigue cracks in forged Ti–6Al–4V. Procedia Eng 2010;2:931–40.
[5] Zhang J, Cheng X, Li Z. Total fatigue life prediction for Ti-alloys airframe structure based on durability and damage-tolerant design concept. Mater Des 2010;31:4329–35.
[6] Stoschka M, Tan W, Eichlseder W, Stockinger M. Introduction to an approach based on the $(\alpha + \beta)$ microstructure of elements of alloy Ti–6Al–4V. Procedia Eng 2009;1:31–4.
[7] Pilchak AL, Williams REA, Williams JC. Crystallography of fatigue crack initiation and growth in fully lamellar Ti–6Al–4V. Metall Mater Trans A 2010;41:106–24.
[8] Oguma H, Nakamura T. The effect of microstructure on very high cycle fatigue properties in Ti–6Al–4V. Scr Mater 2010;63:32–4.
[9] Chan KS. Changes in fatigue life mechanism due to soft grains and hard particles. Int J Fatigue 2010;32:526–34.
[10] Zuo JH, Wang ZG, Han EH. Effect of microstructure on ultra-high cycle fatigue behavior of Ti–6Al–4V. Mater Sci Eng A 2008;473:147–52.
[11] Szczepanski CJ, Jha SK, Larsen JM, Jones JW. Microstructural influences on very-high-cycle fatigue-crack initiation in Ti-6246. Metall Mater Trans A 2008;39:2841–51.
[12] Hines JA, Lütjering G. Propagation of microcracks at stress amplitudes below the conventional fatigue limit in Ti–6Al–4V. Fatigue Fract Eng Mater Struct 1999;22:657–65.
[13] Nalla RK, Boyce BL, Campbell JP, Peters JO, Ritchie RO. Influence of microstructure on high-cycle fatigue of Ti–6Al–4V: bimodal vs lamellar structures. Metall Mater Trans A 2002;33:899–918.
[14] Niinomi M, Akahori T, Fukunaga K, Eylon D. Fatigue crack initiation and fatigue life prediction of Ti–6Al–4V ELI. In: Boyer RR, Eylon D, Lütjering G, editors. Fatigue behavior of titanium alloys. Warrendale (PA): TMS; 1999. p. 307–14.
[15] Ivanova SG, Biederman RR, Sisson RD. Investigation of fatigue crack initiation in Ti–6Al–4V during tensile-tensile fatigue. J Mater Eng Perform 2002;11:226–31.
[16] Peters M, Lütjering G. Control of microstructure and texture in Ti–6Al–4V. In: Kimura H, Izumi O, editors. Titanium'80 science and technology. New York: AIME; 1980. p. 925–35.
[17] Peters JO, Lütjering G. Comparison of the fatigue and fracture of $\alpha + \beta$ and β titanium alloys. Metall Mater Trans A 2001;32:2805–18.
[18] Ivanova SG, Cohen FS, Biederman RR, Sisson RD. Role of microstructure in the mean stress dependence of fatigue strength in Ti–6Al–4V alloy. In: Boyer RR, Eylon D, Lütjering G, editors. Fatigue behavior of titanium alloys. Warrendale (PA): TMS; 1999. p. 39–46.
[19] Adachi S, Wagner L, Lütjering G. Influence of microstructure and mean stress on fatigue strength of Ti–6Al–4V. In: Lütjering G, Zwicher U, Bunk W, editors. Titanium '84 – science and technology, vol. 4. Oberusel: Deutsche Gesellschaft für Metallkunde; 1985. p. 2139–46.
[20] Oguma H, Nakamura T. The effect of microstructures on interior-originating fatigue fractures of Ti–6Al–4V in gigacycle region. In: Lütjering G, Albrecht J, editors. Ti-2003 science and technology. Weinheim: Wiley-VCH; 2004. p. 1783–90.
[21] Peters M, Gysler A, Lütjering G. Influence of microstructure on the fatigue behavior of Ti–6Al–4V. In: Kimura H, Izumi O, editors. Titanium'80 science and technology. New York: AIME; 1980. p. 1777–86.
[22] Lütjering G, Gysler A. Fatigue. In: Lütjering G, Zwicher U, Bunk W, editors. Titanium '84 – science and technology, vol. 4. Oberusel: Deutsche Gesellschaft für Metallkunde; 1985. p. 2065–83.
[23] Peters M, Gysler A, Lütjering G. Influence of texture on fatigue properties of Ti–6Al–4V. Metall Mater Trans A 1984;15:1597–605.
[24] Morrissey RJ, McDowell DL, Nicholas T. Frequency and stress ratio effects in high cycle fatigue of Ti–6Al–4V. Int J Fatigue 1999;21:679–85.
[25] Bellows RS, Muju S, Nicholas T. Validation of the step test method for generating Haigh diagrams for Ti–6Al–4V. Int J Fatigue 1999;21:687–97.
[26] Nagai K, Yuri T, Umeza O, Ogata T, Ishikawa K, Ito Y, et al. High cycle fatigue properties of Ti–6Al–4V alloys at cryogenic temperatures. In: Froes FH, Caplan IL, editors. Titanium'92 science and technology. Warrendale (PA): TMS; 1993. p. 1827–34.
[27] Broichhausen J, Kann HV. Influence of forging conditions on the fatigue behaviour of Ti6Al4V. In: Jaffee RI, Burte HM, editors. Titanium science and technology. New York: Plenum Press; 1973. p. 1785–99.
[28] Hines JA, Peters JO, Lütjering G. Microcrack propagation in Ti–6Al–4V alloys. In: Boyer RR, Eylon D, Lütjering G, editors. Fatigue behavior of titanium alloys. Warrendale (PA): TMS; 1999. p. 15–22.
[29] Rudinger K, Fischer D. Relationship between primary alpha content, tensile properties and high cycle fatigue behavior of Ti–6Al–4V. In: Lütjering G, Zwicher U, Bunk W, editors. Titanium '84 – science and technology, vol. 4. Oberusel: Deutsche Gesellschaft für Metallkunde; 1985. p. 2123–30.

[30] Nalla RK, Altenberger I, Noster U, Liu GY, Scholtes B, Ritchie RO. On the influence of mechanical surface treatments—deep rolling and laser shock peening—on the fatigue behavior of Ti–6Al–4V at ambient and elevated temperatures. Mater Sci Eng A 2003;355:216–30.

[31] Nakanura T, Oguma H, Shiina T. Influence factors on interior-originating fatigue fractures of Ti–6Al–4V in gigacycle region: focusing on stress ratio and internal environment of material. In: Lütjering G, Albrecht J, editors. Ti-2003 science and technology. Weinheim: Wiley-VCH; 2004. p. 1775–82.

[32] Zuo JH, Wang ZG, Han EH. Fatigue behavior of Ti–6Al–4V alloy in vacuum and at low temperature. Adv Mater Res 2008;41–42:83–90.

[33] Geisendorfer RF. Titanium 6Al–4V plate from prealloyed powder. In: Kimura H, Izumi O, editors. Titanium '80 science and technology. New York: AIME; 1980. p. 2225–35.

[34] Tiley J, Searles T, Lee E, Kar S, Banerjee R, Russ JC, et al. Quantification of microstructural features in α/β titanium alloys. Mater Sci Eng A 2004;372:191–8.

[35] Wang KX, Zeng WD, Shao YT, Zhao YQ, Zhou YG. Quantification of microstructural features in titanium alloys based on stereology. Rare Metal Mat Eng 2009;38:398–403.

[36] Spanrad S. Fatigue crack growth in laser shock peened aerofoils subjected to foreign object damage. PhD thesis. University of Portsmouth; 2011.

[37] Altenberger I, Nalla RK, Sano Y, Wagner L, Ritchie RO. On the effect of deep-rolling and laser-peening on the stress-controlled low- and high-cycle fatigue behavior of Ti–6Al–4V at elevated temperatures up to 550 °C. Int J Fatigue 2012;44:292–302.

[38] Vinogradov A, Kawaguchi T, Kaneko Y, Hashimoto S. Fatigue crack growth and related microstructure evolution in ultrafine grain copper processed by ECAP. Mater Trans 2012;53:101–8.

[39] Janeček M, Nový F, Stráský J, Harcuba P, Wagner L. Fatigue endurance of Ti–6Al–4V alloy with electro-eroded surface for improved bone in-growth. J Mech Behav Biomed 2011;4:417–22.

[40] Mughrabi H, Höppel HW. Cyclic deformation and fatigue properties of very fine-grained metals and alloys. Int J Fatigue 2010;32:1413–27.

[41] Sen I, Gopinath K, Datta R, Ramamurty U. Fatigue in Ti–6Al–4V–B alloys. Acta Mater 2010;58:6799–809.